Resilience Evaluation Method Considering Critical Line Identification of Cascading Failure

Pengcheng Lv
School of Electrical Engineering
Southeast University
Nanjing, China
220205570@seu.edu.cn

Yifei Wang
School of Electrical Engineering
Southeast University
Nanjing, China
wyf@seu.edu.cn*i*

2023 6th International Conference on Energy, Electrical and Power Engineering (CEEPE) | 979-8-3503-4827-9/23/$31.00 ©2023 IEEE | DOI: 10.1109/CEEPE58418.2023.10166461

***Abstract*—With the access of large-scale new energy units, the risk of major blackouts caused by extreme disasters in the power grid increases. In order to realize the resilience assessment of the power grid based on cascading failures, this paper establishes a key link screening method based on the steady-state simulation framework of cascading failures. Based on the cascading failure data model with time sampling, the resilience of the power grid is evaluated according to the resilience assessment method with load shedding as the observation index. Based on the IEEE-30 BUS system, the simulation verification is carried out to obtain the effect of grid resilience improvement.**

Keywords—cascading failure, power system security, power grid resilience, power system economic dispatch

I. INTRODUCTION

In recent years, blackouts caused by extreme disasters have occurred frequently. The reason is that with the increase of renewable energy penetration, the inertia of power system decreases, and the ability of power grid to cope with extreme weather or sudden faults decreases [1]-[4].

The research on the mechanism of blackouts mainly focuses on the development of cascading failures in power grids. In recent years, with the increase of renewable energy penetration in the power grid. In recent years, with the increase of renewable energy penetration in the power grid, the randomness of the power grid is enhanced, the power electronics is improved, and the risk of power grid cascading failure is greatly increased [5]–[9]. In order to analyze cascading failures, researchers have proposed many cascading failure simulation models. References [10], [11] proposed the OPA model based on the line overload outage mechanism, and considered the long-time slow process such as the load of power grid and the change of power plants, the new transformation of transmission lines, and the fast process such as scheduling and relay protection during cascading failures.

At present, the concept of 'engineering resilience' has been widely used in multi-engineering disciplines involving the interaction between human and nature, such as engineering technology, organizational behavior, disaster management and environmental evolution response. In recent years, with the increasing frequency of large-scale faults caused by extreme natural disasters, resilience has received increasing attention in power systems.

Power system resilience refers to the ability of the power grid to reduce the loss of the fault process and restore to the normal power supply state as soon as possible in the case of major disasters. A resilient power system can gradually reduce its capacity and quickly return to its original state when external disasters intensify. At present, the research on power grid resilience evaluation is still in its infancy, and there are few related results. On the one hand, according to the occurrence characteristics of extreme natural disasters such as typhoon, rainstorm, earthquake and ice disaster, the mathematical model is established to evaluate the fault probability of power grid components under a certain degree of natural disasters [12], [13]. On the other hand, risk assessment establishes a mathematical model of power outage risk after disasters [14], [15], and analyzes the possibility and impact of large-scale power outages.

In order to realize the resilience evaluation of power grid based on cascading failures, the second chapter of this paper establishes a key link screening method based on the steady-state simulation framework of cascading failures. The third chapter is based on the cascading failure data model using time sampling, and the resilience of the power grid is evaluated according to the resilience evaluation method with load shedding as the observation index. The fourth chapter performs simulation verification to obtain the effect of grid resilience improvement.

II. WEAK LINK IDENTIFICATION OF CASCADING FAILURE

A. A Blackout Simulation Model Considering Multiple Fault Modes

The power system cascading failure model proposed in this section mainly through multiple cascading failure simulations, so that the obtained cascading failure data has certain statistical significance. The specific simulation steps are as follows:

1) Initialize the power system network parameters.

2) The line fault caused by bad weather is sampled and set as the initial fault of the system.

3) Detect whether there is an island in the system, if there is no island, continue to sample the fault line; if there is only one island, then step 4); if the number of islands is greater than or equal to two, then step 6.

4) Calculate the power flow according to the new system topology, and judge whether the power flow of each line is overloaded. For overload lines, the fault probability is calculated according to the fault probability model in formula (1). Thus the line state information is updated.

$$\mathrm{Pr}_l^{trip} = \begin{cases} 1, & p_l \geq p_l^{\lim} \\ \dfrac{p_l - p_l^{rated}}{p_l^{\lim} - p_l^{rated}}, & p_l^{rated} < p_l < p_l^{\lim} \\ 0, & p_l \leq p_l^{rated} \end{cases} \quad (1)$$

where Pr_l^{trip} is the fault probability of line l, p_l is the current load rate of line l, p_l^{rated} is the rated load rate of line l, $p_l^{\lim}$ is the limit load rate of line l. If a new line has overload fault, judge the number of islands. If it is still one, repeat Step 4; if it is greater than or equal to two, proceed to Step 6. If there is no overload fault of new circuit, then enter step 5.

$$t_i = a_i + b_i(1 - e^{-c_i x}), x \geq 0 \quad (2)$$

where, t_i is the time from the previous broken line to the i-th broken line, which is obtained by adding an inherent time a_i and an exponential distribution with b_i as the time coefficient $1/c_i$ as the expected value.

5) Conduct line hidden failure sampling to determine whether hidden failures happen. If new hidden faults occur, enter step 4. If no hidden fault occurs, the optimal cutting load solution will be evaluated. The objective of this model is to minimize the total cutting load under the constraints of power balance and line power flow. At this point, this cascading failure chain has been obtained, and the number of cascading failure simulations is increased by 1. Enter step 7.

6) For each island, determine the type of island. For the number and type of nodes in each island, cut the load, calculate and record the total load loss into step 7.

7) System recovery sampling. For the disconnected line after the fault, the recovery time is set as shown in Equation (3). After the fault development process, the line recovery and load shedding recovery are performed. Cascading failure simulation ends, the number of simulations plus 1 into step 8.

$$t_{ri} = a_{ri} + b_{ri}(1 - e^{-c_{ri} x}), x \geq 0 \quad (3)$$

8) If the number of cascading failure simulations is less than the maximum number of simulations, then enter Step 2. Otherwise, the simulation is completed. The relevant data such as fault lines, machine cutting number, load loss and the fault development curve in each simulation are calculated and recorded.

According to the above description, the simulation flow chart is shown in Figure 1.

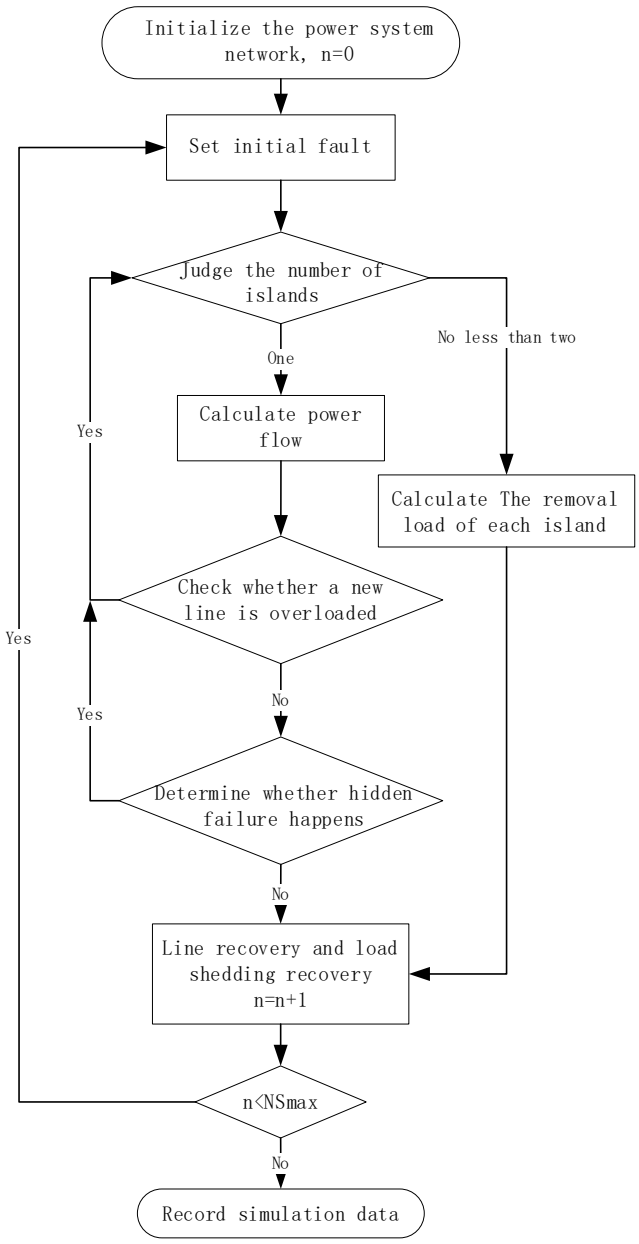

Fig. 1. Cascading failure simulation flow chart

B. Weakness Identification

In order to obtain the key links of the power system in the cascading failure accident chain, it is necessary to screen all lines according to different indicators. After the simulation of the cascading failure accident chain data, these data are processed and the required identification indicators are calculated.

Firstly, the propagation line is defined as the line that causes other line faults in the chain fault propagation relationship, which has the effects of worsening the fault degree and expanding the fault scale. Similarly, the vulnerable line is defined as the line that is affected by other fault lines in the cascading failure propagation relationship, which is susceptible to other fault lines.

For n lines $\bar{v}=\{l_1,l_2,\cdots,l_n\}$ in the power system, the propagation relationship of N fault chain $\{L_1,L_2,\cdots,L_N\}$ through N simulations is represented by undirected graph $\overline{G}=\left(\overline{V}_h,\overline{V}_a,\overline{E}\right)$, that is,

$$\begin{cases}\overline{V}_h=\left\{l_h \mid l_h\in\bar{v},O\left(l_h\right)>0\right\}\\ \overline{V}_a=\left\{l_a \mid l_a\in\bar{v},I\left(l_a\right)>0\right\}\\ \overline{E}=\left\{\left(l_h,l_a\right) \mid l_h\to l_a\right\}\end{cases} \tag{4}$$

where l_h is the transmission line, l_a stands for fragile line. $l_h\to l_a$ stands for propagation relationship, indicates that the failure of line l_h leads to the failure of line l_a. $\overline{V}_h$ represents the set of propagation lines, its element is all the lines with degree $O>0$ in the fault chain. $\overline{V}_a$ represents the fragile fault set, its element is all the lines in the fault chain with degree $I>0$. $\overline{E}$ is the set of edges in an undirected graph $\overline{G}$. The elements are all propagation relationships in the fault chain.

By solving the dimensions of the vectors $\overline{V}_h$ and $\overline{V}_a$, the number of propagation lines n_1 and the number of fragile lines n_2 can be obtained. Propagation probability matrix can be obtained by calculating the proportion of each propagation relation in all fault chains. The probability of failure of l_h in undirected graph G resulting in failure of l_a can be expressed as:

$$\overline{W}(l_h,l_a)=\frac{N_{l_h\to l_a}}{N} \tag{5}$$

where $\overline{W}\in R^{n_1\times n_2}$ is the propagation probability matrix, $N_{l_h\to l_a}$ represents the number of times that the propagation relation $l_h\to l_a$ appears in all faults, and N represents the total number of fault chains.

The value of $\overline{W}(l_h,l_a)$ reflects the frequency of propagation relation $l_h\to l_a$ in the process of interlocking fault propagation. The larger the value is, the more frequently it propagates or the higher the probability of this propagation relationship occurring in cascading failures. If $\overline{W}(l_h,l_a)$=0, it means that the propagation relationship does not exist or its probability is very low.

According to the meaning of the propagation probability matrix $\overline{W}$, each row is the probability that each propagation line leads to the failure of each fragile line. Similarly, each column is the probability that each fragile line is affected by each propagation line. Therefore, the propagation probability matrix is normalized by row normalization and column normalization, and the corresponding row normalization matrix $\overline{W_r}$ and column normalization matrix $\overline{W_c}$ are obtained. Each element in the row normalization matrix $\overline{W_r}$ is the modulus of each element in the original matrix divided by the row vector of the row, and each element in the column normalization matrix $\overline{W_c}$ is the modulus of each element in the original matrix divided by the column vector of the column.

On this basis, the propagation value coefficient matrix $\overline{H}\in R^{n_1\times n_1}$ and vulnerability value coefficient matrix $\overline{A}\in R^{n_2\times n_2}$ can be obtained by using formula (6).

$$\begin{cases}\overline{H}=\overline{W}_r\overline{W}_c^T\\ \overline{A}=\overline{W}_c^T\overline{W}_r\end{cases} \tag{6}$$

The coefficient matrix of vulnerability value obtained in formula (6) can reflect the correlation of fragile lines in the propagation process of chained faults. Specifically, the value of $\overline{A}_{ij}$ represents the probability of failure due to the influence of the same transmission line for both vulnerable line l_i and vulnerable line l_j. The greater the value of A, the greater the probability of failure due to the influence of the same transmission line. In other words, the greater the probability that the fragile line is affected by the same propagation line.

Therefore, the correlation index of cascading failure vulnerable lines can be obtained by formula (7).

$$\bar{a}_{i,j}=\overline{A}_{l_i,l_j}+\overline{A}_{l_j,l_i} \tag{7}$$

where $i,j\in\{1,2,\cdots,n\},i\neq j$. If line l_i and line l_j are not fragile lines, or do not have propagation relations with other lines, the corresponding values of $\overline{A}_{l_i,l_j}$ and $\overline{A}_{l_j,l_i}$ are zero.

Considering that if the N-1 constraint is added to all lines of the power system optimal scheduling model, the feasibility of real-time scheduling for large power systems is low due to the large amount of calculation. Therefore, using the key links selected in this chapter, several faults that have the greatest impact on the cascading failure propagation of the power system are selected. The N-1 security constraints based on the identified key links are established, and the line pairs with the highest correlation are selected to establish N-2 security constraints.

III. Resilience Assessment Based on Cascading Failure Model

To reflect the resilience and safety performance of the power system to extreme disaster events, it is necessary to consider the impact of disaster events to construct power system resilience evaluation indicators and evaluation methods.

According to the typical disaster process system function curve used to describe the system resilience. Fig. 1 shows the typical resilience curve of power system; t_0 is the starting time of disaster events; t_1 is the time of forced outage, t_5 is the time when the system function returned to normal. According to different time stages, the resilience curve can be

divided into adaptability, absorption and recovery. Adaptability refers to the degree to which the system maintains its established functions in the early stage of disaster development; absorption refers to the degree of fault absorption and deterioration during the development of system faults; system resilience refers to the degree and speed of system recovery to normal state, and different time stages constitute the resilience curve and resilience evaluation index.

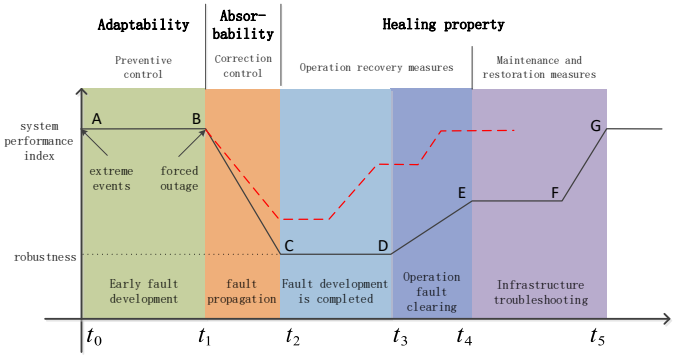

Fig. 2. Resilience index curve

When the system failure enters the propagation stage, the emergency cycle enters the response stage due to the decline of power grid performance. From the initial performance $Q(t_1)$ decline to the minimum performance $Q(t_2)$, the ability to maintain the performance through fault development to t_3, then it enters the maintenance stage. With the recovery of grid components from t_3 to t_4, the performance index rises. Then, until t_5, maintenance and repair measures were taken to restore the power grid to the pre-failure operation state

The total load of the system is taken as an example of system performance index. According to the situation of system load loss shown in the resilience index curve, the factors affecting the power failure time include power failure amount and power failure time. The load change obtained based on a large number of simulation data, according to the missing area of the curve, the comprehensive consideration of power failure amount and power failure time also reflects the specific development process of power failure event.

The index considering the overall resilience of the grid can be characterized by the cumulative performance loss when the grid system performance declines:

$$\begin{aligned} R_{14} &= \int_{t_1}^{t_4} [Q(t_1) - Q(t)]dt \\ &= \int_{t_1}^{t_2} [Q(t_1) - Q(t)]dt + \int_{t_2}^{t_3} [Q(t_1) - Q(t_2)]dt + \int_{t_3}^{t_4} [Q(t_1) - Q(t_2)]dt \end{aligned} \tag{8}$$

The smaller the R_{14}, the less loss of power grid performance, the better the initial.

In order to realize the effect of cascading failure screening, the corresponding N-1 or N-2 constraints are established for the key links proposed above to solve the initial operating point of cascading failure of power grid. Then, according to this toughness evaluation method, the toughness optimization effect of power grid after adding cascading failure constraints is obtained.

IV. Case Studies

In order to realize the screening of key lines and line pairs of cascading failures, establish corresponding safe operation constraints, and realize the verification of resilience improvement, simulation experiments are carried out based on ieee-30 bus system.

The cascading failure simulation of IEEE 30-bus system is carried out, and the maximum number of simulation *NSmax* is 4000, which is to simulate 2000 line sudden fault scenarios. The initial load power coefficient of the system P_D^{coe} is set to 2.5, indicating that the system load is 2.5 times the default load. The line power flow upper limit coefficient of the system is set to 0.8, which indicates that the line power flow upper limit of the system is the default value of the system. The rated load rate p_l^{rated} of the line is taken as 0.9, and the limit load rate of the line $p_l^{\lim}$ is taken as 1.3.

In order to achieve the purpose of simulation verification, this paper designs two examples:

Example 1: Key link screening of cascading failure in ieee-30 bus system;

Example 2: Comparison of resilience improvement after optimal operation of power grid

A. Key Link Screening of Cascading Failure

After the *NSmax*=4000 cascading failure accident chain simulation, according to the data processing and index calculation method described in the text, the comprehensive index of each line is obtained as shown in Figure 2, and 10 lines with the largest comprehensive index are selected as shown in Table I. The selected cascading failure line pairs are shown in Table II.

TABLE I. Line Comprehensive Index Value

Sort	1	2	3	4	5
Line number	10	35	39	20	12
Index value	10.321	7.918	6.100	5.620	5.530
Sort	6	7	8	9	10
Line number	30	9	32	18	40
Index value	5.162	4.982	4.794	4.590	4.355

TABLE II. Sorting of System Related Lines

Sort	1	2	3	4	5
Line pair	10-39	20-39	18-20	32-40	10-13
Index value	1.5499	1.4048	1.3897	1.2214	1.1773

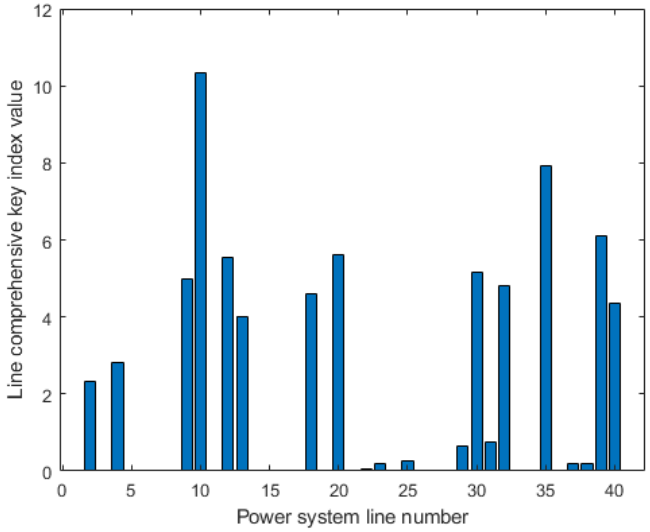

Fig. 3. Line comprehensive index ranking

From Figure 3, it can be seen that some lines are less involved in the cascading failure of the line, while the lines in Table I are very vulnerable to other line disconnections and induce other related lines to disconnect. For this part of the line, establish N-1 constraints. Similarly, the screening of critical line pairs is used to establish N-2 constraints.

B. Resilience Evaluation of Power Grid Optimal Operation

According to the key lines and line pairs selected by example 1, the corresponding N-1 and N-2 constraints are established, and the initial operating state of the power grid is re-solved, and the cascading failure simulation of the same *NSmax* times is carried out. According to the resilience evaluation method described in Chapter 3, the resilience curves of the power grid before and after optimization are evaluated and calculated, as shown in Figure 3 and Figure 4.

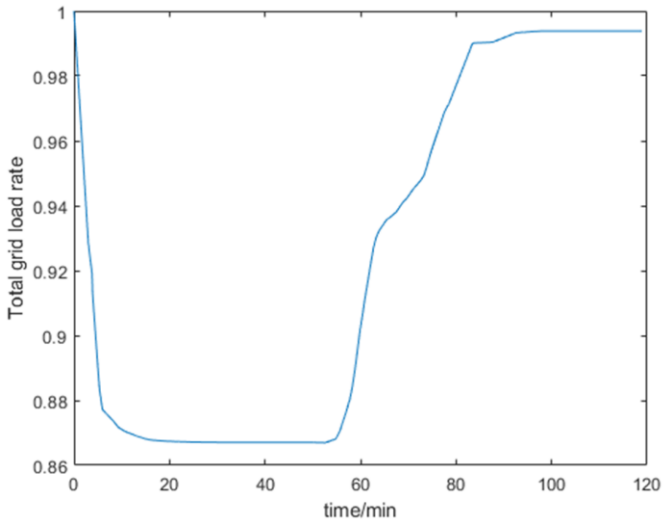

Fig. 4. Resilience curve before optimization

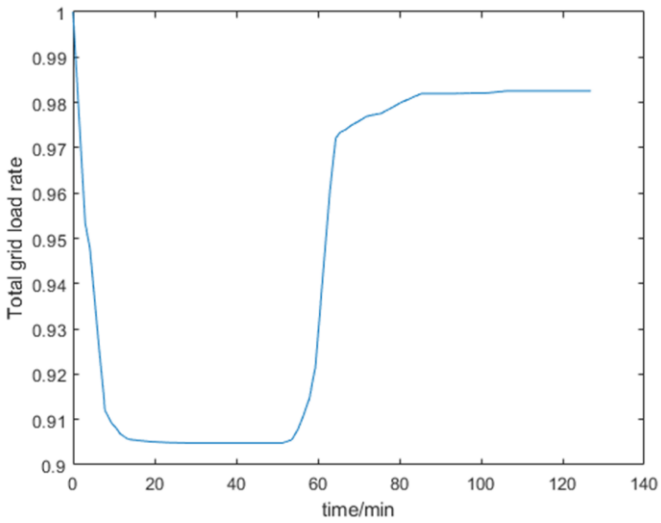

Fig. 5. Resilience curve after optimizationine

Through the comparison of the two curves in Fig. 3 and Fig. 4, it can be seen that after adding N-1 and N-2 constraints after the screening of key lines, the load shedding under failure of the power grid is significantly reduced. The lowest load point rises from 0.8670 to 0.9048, and the resilience index R_{14} decreases from 7.0656 to 4.9487, which proves that adding constraints based on cascading failures from the grid operating point effectively improves the grid resilience.

V. Conclusion

In this paper, based on the established cascading failure simulation model with time sampling, the key links of cascading failure are screened, and the resilience of power grid is evaluated based on simulation data. Then, the grid operation constraints are added through the selected key links, and the simulation verification is carried out in the test system. It is proved that the grid resilience is significantly improved after the N-1 and N-2 constraints are established according to the screening of key links.

Acknowledgment

This paper is supported by National Natural Science Foundation of China (52007032), Basic Research Program of Jiangsu Province (BK20200385).

References

[1] B. A. Carreras, D. E. Newman, I. Dobson, and A. B. Poole, “Evidence for Self-Organized Criticality in a Time Series of Electric Power System Blackouts,” IEEE Trans. Circuits Syst. Regul. Pap., vol. 51, no. 9, pp. 1733–1740, Sep. 2004, doi: 10.1109/TCSI.2004.834513.

[2] B. A. Carreras, V. E. Lynch, D. E. Newman, and I. Dobson, “Blackout mitigation assessment in power transmission systems,” in 36th Annual Hawaii International Conference on System Sciences, 2003. Proceedings of the, Big Island, HI, USA, 2003, p. 10 pp. doi: 10.1109/HICSS.2003.1173911.

[3] A. Khaw, Y. Lim, and J. Wong, "Feasibility of Continues Operation of Photovoltaic Systems with Energy Storage during Grid Outages," International Journal of Electrical and Electronic Engineering & Telecommunications, Vol. 7, No. 1, pp. 1-6, January 2018. Doi: 10.18178/ijeetc.7.1.1-6

[4] N. Khoa, M. Cuong, H. Cuong, and N. Hieu, "Performance Comparison of Impedance-Based Fault Location Methods for Transmission Line," International Journal of Electrical and Electronic Engineering & Telecommunications, Vol. 11, No. 3, pp. 234-241, May 2022. Doi: 10.18178/ijeetc.11.3.234-241

[5] Vaiman et al., "Risk Assessment of Cascading Outages: Methodologies and Challenges," IEEE Trans. Power Syst., vol. 27, no. 2, pp. 631–641, May 2012, doi: 10.1109/TPWRS.2011.2177868.

[6] J. Yan, Y. Tang, H. He, and Y. Sun, "Cascading Failure Analysis With DC Power Flow Model and Transient Stability Analysis," IEEE Trans. Power Syst., vol. 30, no. 1, Art. no. 1, Jan. 2015, doi: 10.1109/TPWRS.2014.2322082.

[7] J. Xu, R. Yao, and F. Qiu, "Mitigating Cascading Outages in Severe Weather Using Simulation-based Optimization," IEEE Trans. Power Syst., pp. 1–1, 2020, doi: 10.1109/TPWRS.2020.3008428.

[8] B. Li, K. Barker, and G. Sansavini, "Measuring Community and Multi-Industry Impacts of Cascading Failures in Power Systems," IEEE Syst. J., vol. 12, no. 4, Art. no. 4, Dec. 2018, doi: 10.1109/JSYST.2017.2768603.

[9] S. V. Buldyrev, R. Parshani, G. Paul, H. E. Stanley, and S. Havlin, "Catastrophic cascade of failures in interdependent networks," Nature, vol. 464, no. 7291, Art. no. 7291, Apr. 2010, doi: 10.1038/nature08932.

[10] Shengwei Mei, Yixin Ni, Gang Wang, and Shengyu Wu, "A Study of Self-Organized Criticality of Power System Under Cascading Failures Based on AC-OPF With Voltage Stability Margin," IEEE Trans. Power Syst., vol. 23, no. 4, pp. 1719–1726, Nov. 2008, doi: 10.1109/TPWRS.2008.2002295.

[11] I. Dobson, B. A. Carreras, V. E. Lynch, and D. E. Newman, "An initial model fo complex dynamics in electric power system blackouts," in Proceedings of the 34th Annual Hawaii International Conference on System Sciences, Maui, HI, USA, 2001, pp. 710–718. doi: 10.1109/HICSS.2001.926274.

[12] G. Huang, J. Wang, C. Chen, J. Qi, and C. Guo, "Integration of Preventive and Emergency Responses for Power Grid Resilience Enhancement," IEEE Trans. Power Syst., vol. 32, no. 6, pp. 4451–4463, Nov. 2017, doi: 10.1109/TPWRS.2017.2685640.

[13] C. Chen, J. Wang, F. Qiu, and D. Zhao, "Resilient Distribution System by Microgrids Formation After Natural Disasters," IEEE Trans. Smart Grid, vol. 7, no. 2, pp. 958–966, Mar. 2016, doi: 10.1109/TSG.2015.2429653.

[14] Y. Wang et al., "A Resilience Assessment Framework for Distribution Systems Under Typhoon Disasters," IEEE Access, vol. 9, pp. 155224–155233, 2021, doi: 10.1109/ACCESS.2021.3128967.

[15] H. Sabouhi, A. Doroudi, M. Fotuhi-Firuzabad, and M. Bashiri, "Electrical Power System Resilience Assessment: A Comprehensive Approach," IEEE Syst. J., vol. 14, no. 2, pp. 2643–2652, Jun. 2020, doi: 10.1109/JSYST.2019.2934421.